**INTERNATIONAL JOURNAL
ON INFORMATICS VISUALIZATION**

INTERNATIONAL
JOURNAL ON
INFORMATICS
VISUALIZATION

Comparison Analysis of CXR Images in Detecting Pneumonia Using VGG16 and ResNet50 Convolution Neural Network Model

Nur Izdihar [a], Syarifah Bahiyah Rahayu [a,b,*], K.Venkatesan [a,b]

[a] *Department of Science Defense, Faculty of Defense Science and Technology, National Defence University Malaysia (UPNM).*
[b] *Cyber Security and Digital Industrial Revolution Centre, National Defence University Malaysia (UPNM).*
Corresponding author: [*]syarifahbahiyah@upnm.edu.my.

Abstract—**Pneumonia is a lung disease that causes serious fatalities worldwide. Pneumonia can be complicated for medical professionals to identify since it shares similarities with other lung diseases like lung cancer and cardiomegaly. Hospitals face difficulty finding professional radiologists who help to detect pneumonia through radioactive processes. This research proposes VGG16 and ResNet50-based system architecture using the Convolutional Neural Network (CNN) module, which allows the detection of pneumonia. This research identifies pneumonia using chest X-ray (CXR) images through VGG16 and ResNet50 of CNN model architectures. The performance of the proposed models is compared by performance parameters such as processing time, accuracy, and loss. The Pneumonia dataset was obtained from Kaggle and divided into 70% for training, 15 % for validation, and 15% for testing. The results show that the proposed ResNet50 model architecture has a better result than the VGG16 model architecture. It can be clearly observed based on both models' loss and accuracy results. Moreover, the processing time for ResNet50 in training and predicting the CXR images is much faster than the VGG16 model's processing time. Hence, ResNet50 performs better than VGG16 based on the result of loss and accuracy and the processing time for the model to train and predict the data. In conclusion, the findings show the capability of CNN models for detecting pneumonia in CXR images, thus reducing the burden of professional radiologists.**

Keywords—**Pneumonia; CXR images; convolutional neural network; classifier; image enhancement.**

I. INTRODUCTION

Pneumonia is the most infectious, which causes death for children under five, accounting for 14 percent of all fatalities in infants and toddlers under five in 2019. As per the World Health Organization (WHO) (2021), people 65 years old or older, as well as people with pre-existing health conditions, are highly susceptible to pneumonia W.H.O[1]. Guidelines have suggested detecting pneumonia in hospital settings with a chest x-ray (CXR) imaging or other related radioscopy assessment. When people breathe in viruses and bacteria from their nasal or throat, these harmful microorganisms can enter the lungs and cause pneumonia [2]. Droplets from sneezing or coughing might also disperse viruses through the air. WHO stresses the importance of ensuring an individual's nutrition and addressing environmental factors such as air pollution, which should be considered seriously to reduce the number of individuals infected by pneumonia. Pneumonia, explicitly focusing on definite Community-Acquired Pneumonia (CAP), is a condition in which the tissues on one or both sides of the lungs become inflamed due to a virus, bacterial infection, or fungus infection. Streptococcus pneumonia, followed by Haemophilus influenza type b (Hib), is the primary cause of bacterial pneumonia infection in children. WHO describes pneumonia as an acute respiratory illness primarily affecting the lungs. For patients, pneumonia fills the lungs' alveoli with pus and fluid, making breathing difficult and limiting oxygen intake.

One standard indicator of CAP is a body temperature exceeding 38 degrees Celsius or falling below 36 degrees Celsius, accompanied by shaking, sweating, chest pain, chills, a new cough, or sudden difficulty breathing [3]. Furthermore, pneumonia can spread through the blood easily during and immediately after birth. Inadequate nutrition and poor environmental management are risk factors for pneumonia morbidity, particularly in children. Hence, medical experts need to take advantage of telemedicine, which, in this case, detects pneumonia and assists in its diagnosis.

As per discussion by Mehta T [4], pneumonia has the most considerable fatality rate among infectious illnesses and is the

third leading cause of death. The longer it takes to get a proper diagnosis, the more likely it leads to death. As a result, rapid detection is an essential process. Current pneumonia detection is primarily based on the patient's physical symptoms and CXR images from the medical imaging department [5]. Even with CXR images, medical experts still need to analyze each image carefully to diagnose the patient. This procedure seems fine and practicable; however, it can be quite a hassle for medical experts to carefully examine the CXR when hundreds of patients wait to be diagnosed [6]. The main objective of this research is to identify pneumonia disease based on the CXR images using VGG16 and ResNet50 of CNN model architectures. Furthermore, the performance of this work is evaluated for VGG16 and ResNet50 based on processing time, accuracy, and loss.

CNN forms the backbone of modern computer vision systems and has revolutionized the field of image processing. At their core, CNN are designed to automatically learn hierarchical patterns and features from input images without needing handcrafted features, making them highly effective in image recognition tasks. The CNN models consist of a combination of convolutional, pooling, and fully connected layers. This allows CNN to process images hierarchically, learning increasingly complex features from low-level edges and textures to high-level object representations [7]. The hierarchical feature learning is the crucial factor behind CNN's exceptional effectiveness in tasks such as image recognition[8], object detection[9], segmentation [10], and image extraction [11].

CNN has demonstrated remarkable success in medical image classification tasks, such as identifying diseases based on medical images. For example, CNNs can accurately distinguish between normal and abnormal X-rays [12], tuberculosis [13], lung cancer [14], and covid-19 [15], and brain tumor detection [16]. In radiology, CNNs have been employed for accurate and efficient detection of abnormalities in mammograms [17], aiding in early breast cancer detection.

Conventional methods and extraction of features use support vector machine (SVM) [18], logistic regression [19], and random forest [20]. These algorithms effectively analyze the pattern with mining EHR datasets [21]. Even though the conventional methods are simple to work, it cannot perform high-dimensional datasets. Furthermore, data labeling reliability is sometimes challenging and impractical [22]. Advanced modeling uses deep learning algorithms such as convolutional neural networks (CNN) and recurrent neural networks (RNN) to overcome these limitations. Furthermore, CNN has been employed to detect pneumonia. In [23], Avola et al. propose 12 different CNN model architectures in their study, which include MobileNet V2, MobileNet V3, ResNet50, Wide ResNet50, and VGG16, which resulted in an accuracy of 82.0%, 81.0%, 78.0%, 68.0%, and 72.0% respectively. The authors in [24] proposed CNN with ResNet network architecture with five different layer counts: 18, 34, 50, 101, and 152. The authors also enhance another ResNet model, the customized DTL ResNet18. The ResNet network's six members achieved accuracy rates of 91.4%, 90.8%, 92.6%, 92.9%, 92.9%, and 94.7%, respectively.

In addition, Gayathri et al.[25] found two models for feature extraction were introduced, one of which is an ensemble of Inception ResNet V2. The features are then processed through a custom-created sparse autoencoder to reduce the dimensionality of the feature vector before being classified using a feed-forward neural network (FFNN). The feature extraction, dimensionality reduction, and classification stages were proposed as the three steps. The accuracy of Inception ResNet V2 is 91.49%. In [26], the author proposed a different technique where the authors compared the accuracy of 17 different individual CNN model architectures and one (1) model that combined all 17 CNNs with five types of classifiers. The accuracy of VGG16, ResNet18, MobileNet V2, VGG19, InceptionResNet V2, ResNet50, ResNet101, and the 17 combined CNNs is 94.34%, 94.47%, 93.73%, 94.42%, 93.82%, 93.71%, 92.96%, 99.62% respectively.

The author Musallam et al. in[27] proposed their model known as "DeepChest" and compared it with three commonly used CNN models, which are VGG16, DenseNet-121, and MobileNet. VGG16, MobileNet, and "DeepChest" resulted in an accuracy of 93.65%, 94.69%, and 96.56%, respectively. In [28], Fenglin et al. proposed MobileNetV2 and VGG16 as the CNN model architectures. The accuracy for the 4-class category that combined COVID-19, Healthy, Pneumonia Bacterial, and Pneumonia Viral was 87.74% and 87.39%, respectively, for MobileNetV2 and VGG16. In contrast, the accuracy for the 3-class category that combined COVID-19, Healthy, and Pneumonia (Viral + Bacterial) was 96.03% and 95.67%, respectively.

The rest of this paper is organized as follows. Section 2 explains the research methodology of this proposed research work and the training procedure involved in CNN. Section 3 describes a brief finding of this experiment and its results. Section 4 describes the conclusion and future scope of this research work.

II. MATERIALS AND METHOD

This study proposes two CNN architecture models, namely ResNet50 and VGG16. These two CNN architecture models are then paired with a prediction classifier. ResNet50 is a 50-layer convolutional neural network consisting of 48 convolutional layers, one MaxPool layer, and one average pool layer. Artificial neural networks (ANNs) that use residual blocks to build networks are known as residual neural networks. At the same time, VGG16 is a 16-layer convolutional neural network that consists of 3 (three) fully connected layers and 13 (thirteen) convolutional layers. VGG16 receives an image input of 224 x 224. The first two layers are fully connected and have 4,096 channels, whereas the third layer has 1,000. The training is done in 16 epochs with 326 steps each. It is to ensure optimal accuracy and processing time can be achieved. In addition, each CNN model operates separately, one at a time, as it can influence the training process's processing time, accuracy, and loss.

A classifier model is embedded in the Methodology Diagram to identify the images input into its classes. The classification is done by generating a line between the input data and segregating it by its classes. Fig.1 shows the methodology diagram for this research work.
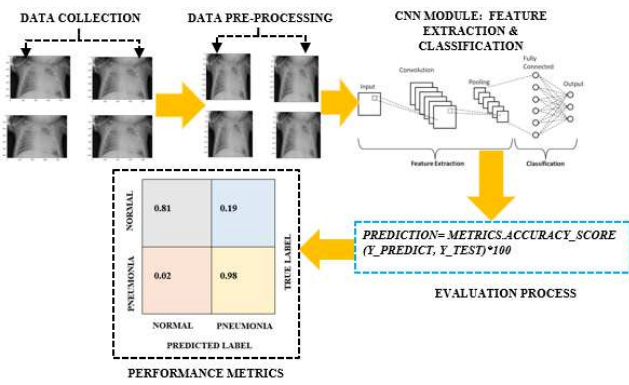
Fig. 1 Methodology Diagram

Thus, this research consists of four main processes: data collection, preprocessing, model development, and evaluation.

A. Data Collection

This proposed methodology begins with the collection of required images for various classes. For this research, the CXR dataset is taken from Kaggle.com. After collecting the dataset from the sources mentioned above, it has been stored locally. This allows performing the dataset training much more accessible. The dataset contains 5,856 CXR images, which consist of standard and pneumonia-infected images. The CXR images are also categorized into three sections: the training dataset, the test dataset, and the validation dataset. It is an advantage for this study that all of the images in the dataset have already been segmented. Hence, the data cleansing process becomes much easier to execute. Table 1 shows the details of the dataset distribution.

B. Data Pre-Preprocessing

As mentioned, the CXR images in this dataset have already been segmented, which is handy for the data preprocessing process. As a result, the CXR images are resized to 224 x 224 pixels during this process to remove any inconsistencies. Moreover, the pixel range of the CXR is modified from 0 to 1 instead of from 0 to 255 by dividing the CXR by 255. The main reason the CXR has been changed in specific ways is to ensure the machine learning process runs smoothly.

C. CNN Model Development

The model development process introduces the concept of creating CNN models to detect pneumonia disease. CNN is a widely used deep learning network because it can convert a multidimensional input visual into a desired output [29]. The model uses ResNet50 and VGG16 CNN model architectures. ResNet50 is a 50-layer convolutional neural network consisting of 48 convolutional layers, one MaxPool layer, and one average pool layer. Artificial neural networks (ANNs) that use residual blocks to build networks are known as residual neural networks [30]. VGG16 is a 16-layer convolutional neural network that consists of 3 (three) fully connected layers and 13 (thirteen) convolutional layers. VGG16 receives an image input of 224 x 224. The first two layers are fully connected and have 4,096 channels, whereas the third layer has 1,000. The training is done in 16 epochs with 326 steps each. It is to ensure optimal accuracy and processing time can be achieved. In addition, each CNN

model operates separately, one at a time, as it can influence the training process's processing time, accuracy, and loss.

The model of the classifier is embedded to recognize distinct patterns and features that differentiate typical lung structures from those affected by pneumonia. These patterns may include the presence of infiltrates, consolidations, and abnormal opacities in pneumonia cases compared to the clear lung fields observed in standard CXR images. Once the training is completed, the classifier enters the prediction phase, where it is presented with new, unseen CXR images. The classifier then applies its learned knowledge and analyzes the image to determine whether it falls into the normal or pneumonia category. To accomplish this, the classifier extracts relevant features from the input image, such as texture, shape, and intensity distributions. These are then processed through the learned model to yield a prediction.

TABLE I
DATASET OF DISTRIBUTION

Dataset	No. of Data	% of Utilization
Training	4,100	70
Validation	878	15
Testing	878	15

D. Performance Measurement

The evaluation process considers processing time, loss, and accuracy. In this study, processing time denotes the duration required for a detection model to finish its tasks or provide its output. This crucial metric assesses the efficiency and effectiveness of the employed models. The measurement of processing time starts at the operation's initiation and concludes upon its finalization, with results expressed in seconds.

The loss of a model is the accumulation of errors in the model. It evaluates the model's performance, which means if the total value of losses is low, the model is performing well, while if the total value of losses is high, the model is not performing as well as intended. Hence, it is essential to ensure that the model's loss is as minimal as possible.

A model's accuracy shows its ability to predict the CXR, whether it is normal or due to pneumonia. The result is very straightforward to analyze. If the value of the accuracy of the model is high, there is a higher confidence that the prediction is accurate. One of the packages in Python, the matplotlib package, is used to evaluate the result. The results are shown in a graph for better visualization. The results are expected to yield two (2) evaluation process graphs, such as the model accuracy and loss graphs.

Next, a confusion matrix is produced. This matrix provides better visualization to observe the performance of the mentioned models. There are a few terms in the confusion matrix, which are true positive (TP), true negative (TN), false positive (FP), and false negative (FN). The processing time, accuracy, recall, precision, and F1-score are also observed to evaluate and conclude which of the two models gives a better result. The accuracy, precision, recall, and F1-score formulas are shown below.

Accuracy = (True Positives + True Negatives) / (True Positives + True Negatives + False Positives + False Negatives)
Precision = True Pos / (True Positives False Positives)

Recall = True Positives / (True Positives + False Negatives)
F1-score = 2 * (Precision * Recall) / (Precision + Recall)

In conclusion, the workflow of our proposed CNN-based VGG16 and ResNet50 architectures starts with inputting CXR images. Then, the images are resized, which helps to perform the subsequent process. The complete labeling for the training of the subsets is declared, and these images are uploaded for the training of the machine-learning model. Once the training process is completed, then the validation and testing phase should proceed. To perform the image classification, i.e., identifying standard and pneumonia images are used. Finally, the evaluation process is performed using the confusion matrix. Fig. 2 shows the workflow of our proposed CNN-based VGG16 and ResNet50 architectures for identifying pneumonia using CXR images.
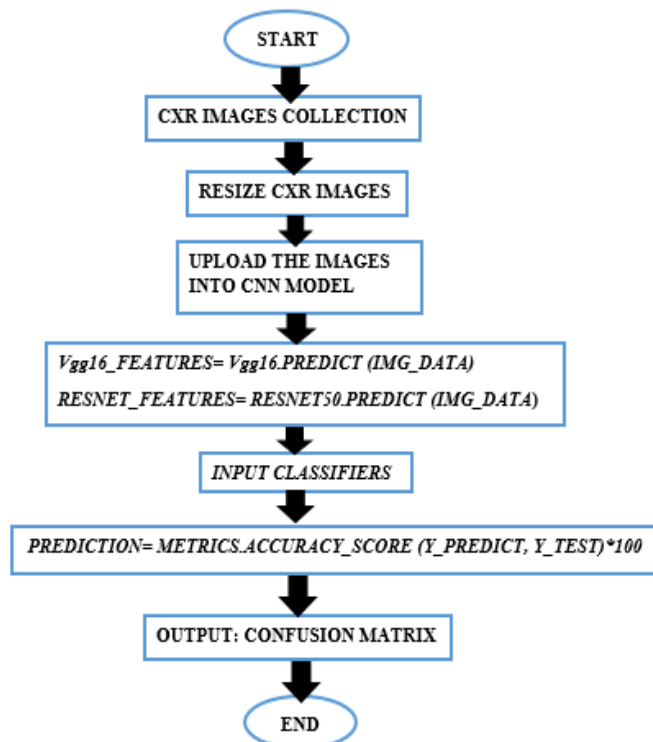

Fig. 2 Flow chart for the proposed method

III. RESULTS AND DISCUSSIONS

This section discusses the results of all training and evaluation processes. We review the loss and accuracy data from the last five (5) epochs of the trained models, as well as the graphs that display the performance of the proposed models. Furthermore, we also examine the graphs of the training models and validation accuracy, overall loss, and accuracy for the VGG16 and ResNet50 CNN models. We also evaluate the test results and compare them for VGG16 and ResNet50 models. Finally, this section elaborates on the challenges and failures encountered during the research process. It is necessary to address these aspects for future studies to have a comprehensive reference.

A. Result of pretrained Models: ResNet50

The last five (5) epochs of the ResNet50 model are listed below:

TABLE II
CLASSIFICATION REPORT RESNET 50 MODEL

Epoch	Duration	4s/stop loss	Accuracy	Value Loss
12/16	1228s	0.0462	0.9833	0.0655
13/16	1241s	0.0560	0.9797	0.0802
14/16	1290s	0.0505	0.9835	0.0802
15/16	1257s	0.0452	0.9835	0.0974
16/16	1234s	0.0422	0.9850	0.0524

Fig 3 shows that the processing time for the data to be trained with the ResNet50 model is 20.83 minutes on average per epoch. Both loss and validation loss are below 11%, which means the accumulation of errors found in the pre-trained model is significantly low. This shows that the pre-trained model is performing well after training the data. Furthermore, the trained model's accuracy and validation accuracy scored above 90%, which is a significantly high value in predicting the CXR image as usual or pneumonia. Next, the results for both loss and accuracy of the trained model have been compiled and displayed in Fig 3 for better visualization.
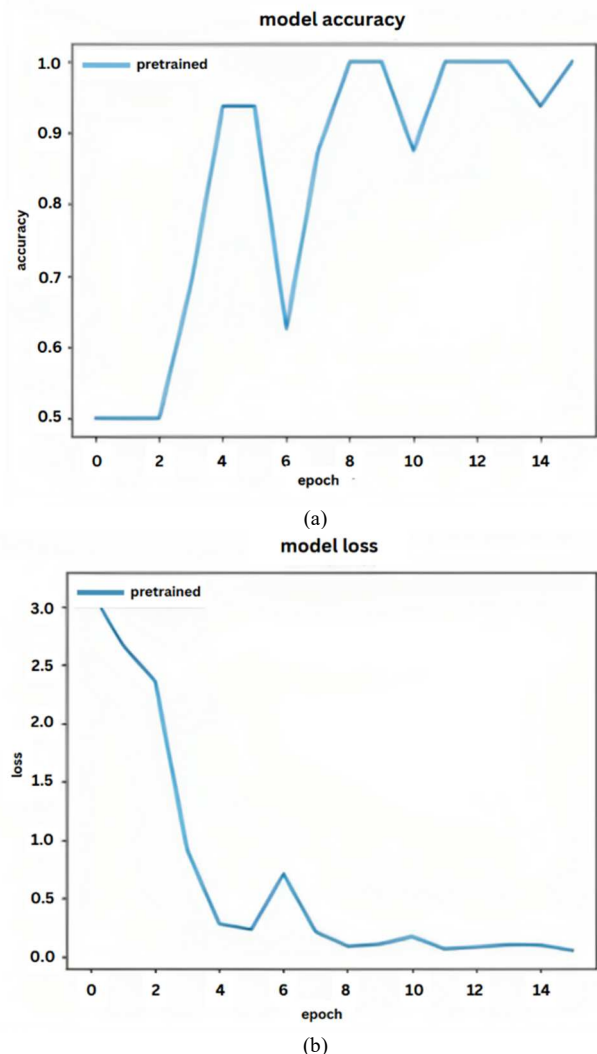

(a)

(b)

Fig. 3 Graph of (a). Accuracy: and (b). Loss of ResNet50 Model

Over each epoch, the accuracy of the trained model rises and reaches 100% accuracy, while the decrement of the loss value for the trained model has gained 0% by the end of the

final epoch, which is the 16th epoch. The findings show the processing time for the model to be thoroughly evaluated is 6.03 minutes. The overall loss is 3.14%, and the accuracy is 99.04%, which shows that the model is performing well as it found only 3.14% errors in the model and can accurately predict the CXR image as usual or pneumonia with an accuracy of 99.04%.

1) Classification and Confusion Matrix: This section provides details regarding the confusion matrix and the classification report, which covers the precision, recall, and F1-score of the ResNet50 model.

TABLE III
CLASSIFICATION REPORT RESNET 50 MODEL

Classification Report	Precision	Recall	F1-score	Support
Normal	0.96	0.81	0.88	234
Pneumonia	0.90	0.98	0.94	390
Accuracy			0.92	624
Macro average	0.93	0.90	0.91	624
Weighted average	0.92	0.92	0.92	624

The processing time for the model to predict the test data is 43 seconds. TABLE III shows that the precision for standard test data is 96 %, while the precision for pneumonia test data is 90 percent. Next, for the recall of the model, standard test data scores 81%, while pneumonia test data scores 98%. Lastly, for the F1-score, standard test data shows 88%, while pneumonia test data scores 94%. Based on the confusion matrix displayed in Fig 6, the outcome for the model to predict standard test data as normal is 81% of accuracy, which is known as the "true positive value," while the outcome for the model to predict pneumonia test data as pneumonia is 98% of accuracy, which is also known as the "true negative value." Next, the outcome for the model that predicts standard test data as pneumonia is 19%. In comparison, pneumonia test data as usual is only 2%, which is noted as false negative and false positive values, respectively. The summary of the confusion matrix is shown in Fig. 5.

Fig. 5 Confusion Matrix of ResNet50 Model

2) Test Evaluation: As mentioned in Section 3, the model is to be tested using a back-end system. Firstly, the test image of CXR is imported first for resizing. The resizing for the CXR image is the same as that for the data pre-processing. The images are resized to 224 by 224 pixels, and the pixel range is set to 0 to 1 by dividing the image by 255 pixels. The CXR image before and after resizing is shown in Fig 4 below:

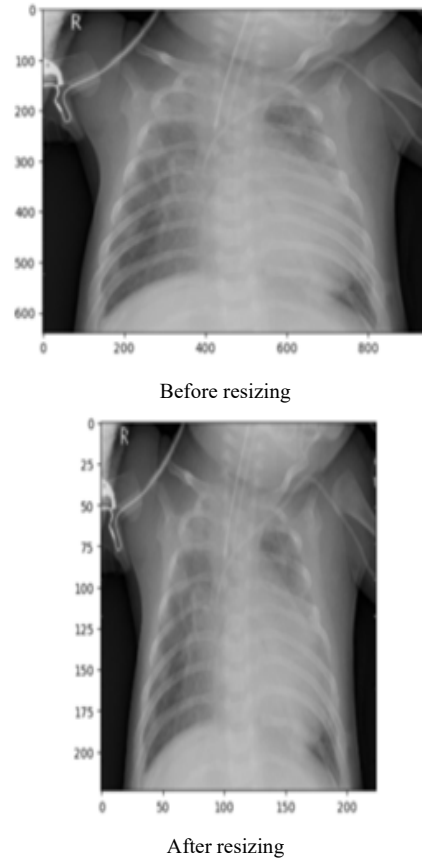
Before resizing

After resizing
Fig. 4 Test CXR for ResNet50

Next, the pre-trained model of ResNet50 predicts the image, and the result indicates the predicted result of the CXR image import is pneumonia, as the loss value is lower than the accuracy value. This shows that the proposed model correctly predicted (95.86%) that the CXR image represents pneumonia.

B. Result of pretrained Models: VGG16

The last five (5) epochs of the VGG16 model are listed below:

TABLE IV
CLASSIFICATION REPORT VGG16 MODEL

Epoch	Duration	9s/stop loss	Accuracy	Value Loss
12/16	2805s	0.0796	0.9691	0.2280
13/16	2832s	0.0738	0.9743	0.2854
14/16	2813s	0.0702	0.9760	0.1874
15/16	2815s	0.0664	0.9753	0.2632
16/16	2808s	0.0748	0.9720	0.2607

Based on the last five (5) epochs of VGG16, as seen in Table IV, the processing time for the data to be trained by the VGG16 model is 46.91 minutes on average per epoch. Both the loss and the validation loss are below 30%. This shows that the pre-trained model is performing well after training the data. Furthermore, the pre-trained model's accuracy and

validation accuracy scored above 90%, which is a significantly high value in predicting the CXR image as usual or pneumonia. The result for both loss and accuracy of the trained model has then been compiled and displayed in Fig.5 below for better visualization.

Fig 5 displays that over each epoch, the accuracy of the trained model reaches over 92%, while the decrement of the loss value for the trained model did not reach 0% by the end of the final epoch, which is the 16th epoch. The overall value for loss and accuracy of the trained model shows that the processing time to evaluate the model is 13.73 minutes. The overall loss is 5.21%, and the accuracy is 98.16%, which indicates that the model is performing very well. It found only 5.21% errors in the model and can accurately predict the CXR image as usual or pneumonia with an accuracy of 98.16%.
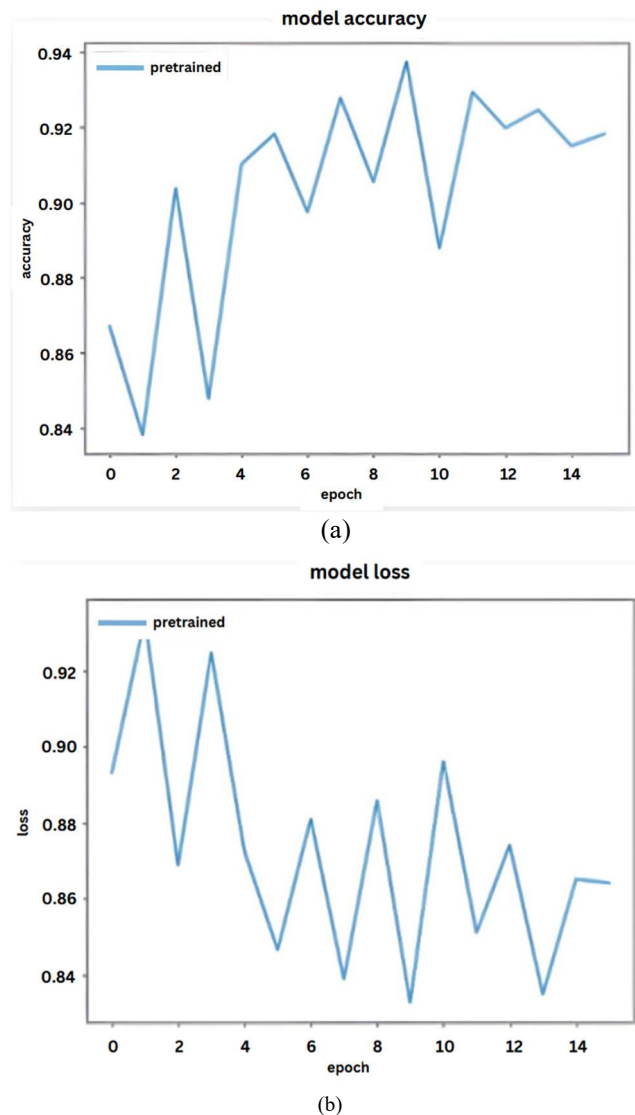

(a)

(b)

Fig. 5 Graph of (a). Accuracy and (b). Loss of VGG16 Model

1) Classification and Confusion Matrix: This part confers in-depth details regarding the confusion matrix and the classification report, which cover the processing time, precision, recall, and F1-score of the VGG-16 model. The processing time for the model to predict the test data is 91 seconds. As can be observed from Table V, the precision for the standard test data is 99%, while the precision for the pneumonia test data is 89%.

Classification Report	Precision	Recall	F1-score	Support
Normal	0.99	0.79	0.88	234
Pneumonia	0.89	0.99	0.94	390
Accuracy			0.92	624
Macro average	0.94	0.89	0.91	624
Weighted average	0.93	0.92	0.92	624

Next, for the recall of the model, standard test data scores 79 percent, while pneumonia test data scores 99%. Lastly, for the F1-score, standard test data shows 88%, while pneumonia test data scores 94%. Based on the confusion matrix displayed, the outcome for the actual positive value is 79%, while the outcome for the true negative value is 99%. On the other hand, the outcome for the model that predicts standard test data as pneumonia is 21%. In comparison, pneumonia test data as standard is only 1%, which are noted as false negative and false positive values, respectively. These results are enlisted in Fig.6.

Fig. 6 Confusion Matrix of VGG16 Model

2) Test Evaluation: As mentioned in section 3, the model is to be tested using a back-end system. As in the previous section mentioned above for the ResNet50 model, the exact process is repeated but uses the VGG16 model. The CXR image before and after resizing is shown in Fig.7 below.
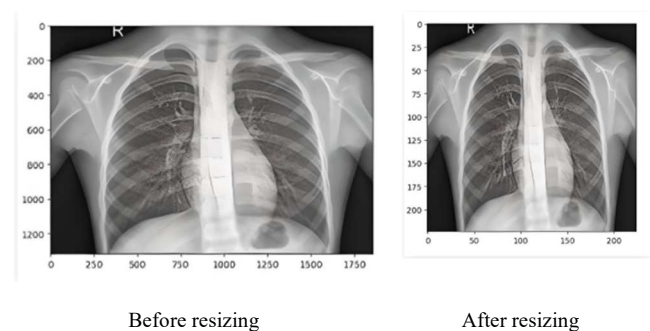

Before resizing   After resizing

Fig. 7 Test CXR for VGG16

Next, the pre-trained model of VGG16 predicts the image and the result is displayed. The predicted result of the CXR image import is standard, as the loss value is greater than the accuracy value. The model is only 7.13% accurate, and the CXR image is of pneumonia. Based on the result displayed and discussed previously in 4.1, the ResNet50 model architecture features a better result than the VGG16 model architecture. It can be clearly observed based on both models'

loss and accuracy results. Moreover, the processing time for ResNet50 in training and predicting the CXR images is much faster than the VGG16 model's processing time. Hence, ResNet50 performs better than VGG16 based on the result of loss and accuracy and the processing time for the model to train and predict the data.

IV. CONCLUSION

This research detailed CNN model-based architecture to detect pneumonia on the CXR image dataset. The significance of this study is to broaden the roles of the medical imaging department to include not only taking images of portions of patients' bodies for diagnostic purposes but also assisting medical experts in interpreting the CXR images by fully utilizing the pneumonia detection system. The proposed approach analyzes CXR images, which will better assist medical experts with diagnosing patients, which in this case is to detect pneumonia. Besides that, the system also reduces the time to analyze the CXR images. The findings of this study are beneficial for expanding the use of computer-aided techniques in medical fields. These techniques can be further developed for analyzing other types of medical imaging, such as CT scans and MRIs. The training process uses VGG16 and ResNet50-based CNN models using 16 epochs with 326 steps each. The result obtained is 99 % accuracy for VGG16 and 98% accuracy for the Resnet50 model. The proposed system is expected to perform better in real-world scenarios and diagnose Pneumonia through CXR images. The future scope of this research is to develop a highly accurate model to detect various types of pneumonia, bacteria, and viruses.

REFERENCES

[1] S. Hassantabar, M. Ahmadi, and A. Sharifi, "Diagnosis and detection of infected tissue of COVID-19 patients based on lung x-ray image using convolutional neural network approaches," *Chaos, Solitons and Fractals*, vol. 140, p. 110170, 2020.

[2] N. Absar *et al.*, "Development of a computer-aided tool for detection of COVID-19 pneumonia from CXR images using machine learning algorithm," *J. Radiat. Res. Appl. Sci.*, vol. 15, no. 1, pp. 32–43, 2022.

[3] K. G. Rögnvaldsson, A. Bjarnason, I. S. Ólafsdóttir, K. O. Helgason, A. Guðmundsson, and M. Gottfreðsson, "Adults with symptoms of pneumonia: a prospective comparison of patients with and without infiltrates on chest radiography," *Clin. Microbiol. Infect.*, vol. 29, no. 1, pp. 108.e1-108.e6, 2023.

[4] T. Mehta and N. Mehendale, "Classification of X-ray images into COVID-19, pneumonia, and TB using cGAN and fine-tuned deep transfer learning models," *Res. Biomed. Eng.*, vol. 37, no. 4, pp. 803–813, 2021.

[5] C. Ieracitano *et al.*, "A fuzzy-enhanced deep learning approach for early detection of Covid-19 pneumonia from portable chest X-ray images," *Neurocomputing*, vol. 481, pp. 202–215, 2022.

[6] N. Sri Kavya, T. shilpa, N. Veeranjaneyulu, and D. Divya Priya, "Detecting Covid19 and pneumonia from chest X-ray images using deep convolutional neural networks," *Mater. Today Proc.*, vol. 64, pp. 737–743, 2022.

[7] B. Ibrokhimov and J.-Y. Kang, "Deep Learning Model for COVID-19-Infected Pneumonia Diagnosis Using Chest Radiography Images," *BioMedInformatics*, vol. 2, no. 4, pp. 654–670, 2022.

[8] A. S. Musallam, A. S. Sherif, and M. K. Hussein, "Efficient framework for detecting COVID-19 and pneumonia from chest X-ray using deep convolutional network," *Egypt. Informatics J.*, vol. 23, no. 2, pp. 247–257, 2022.

[9] M. Abdar *et al.*, "UncertaintyFuseNet: Robust uncertainty-aware hierarchical feature fusion model with Ensemble Monte Carlo Dropout for COVID-19 detection," *Inf. Fusion*, vol. 90, no. September 2022,

pp. 364–381, 2023.

[10] M. Heidari *et al.*, "HiFormer: Hierarchical Multi-scale Representations Using Transformers for Medical Image Segmentation," *Proc. - 2023 IEEE Winter Conf. Appl. Comput. Vision, WACV 2023*, pp. 6191–6201, 2023.

[11] M. Xin and Y. Wang, "Research on image classification model based on deep convolution neural network," *Eurasip J. Image Video Process.*, vol. 2019, no. 1, 2019.

[12] K. Aktas, V. Ignjatovic, D. Ilic, M. Marjanovic, and G. Anbarjafari, "Deep convolutional neural networks for detection of abnormalities in chest X-rays trained on the very large dataset," *Signal, Image Video Process.*, vol. 17, no. 4, pp. 1035–1041, 2023.

[13] J. L. P. Ignatius, S. Selvakumar, K. G. J. L. Paul, A. B. Kailash, S. Keertivaas, and S. A. J. Akarvin Raja Prajan, "Histogram Matched Chest X-Rays Based Tuberculosis Detection Using CNN," *Comput. Syst. Sci. Eng.*, vol. 44, no. 1, pp. 81–97, 2022.

[14] A. A. Shah, H. A. M. Malik, A. H. Muhammad, A. Alourani, and Z. A. Butt, "Deep learning ensemble 2D CNN approach towards the detection of lung cancer," *Sci. Rep.*, vol. 13, no. 1, pp. 1–15, 2023.

[15] A. A. Reshi *et al.*, "An Efficient CNN Model for COVID-19 Disease Detection Based on X-Ray Image Classification," *Complexity*, vol. 2021, 2021.

[16] Y. Anagun, "Smart brain tumor diagnosis system utilizing deep convolutional neural networks," *Multimed. Tools Appl.*, no. 0123456789, 2023.

[17] N. F. Razali, I. S. Isa, S. N. Sulaiman, N. K. Noor, and M. K. Osman, "CNN-Wavelet scattering textural feature fusion for classifying breast tissue in mammograms," *Biomed. Signal Process. Control*, vol. 83, no. November 2022, p. 104683, 2023.

[18] M. Malvoni, M. G. De Giorgi, and P. M. Congedo, "Data on Support Vector Machines (SVM) model to forecast photovoltaic power," *Data Br.*, vol. 9, pp. 13–16, 2016.

[19] P. Ranganathan, C. Pramesh, and R. Aggarwal, "Common pitfalls in statistical analysis: Logistic regression," *Perspect. Clin. Res.*, vol. 8, no. 3, pp. 148–151, 2017.

[20] J. Ali, R. Khan, N. Ahmad, and I. Maqsood, "Random forests and decision trees," *IJCSI Int. J. Comput. Sci. Issues*, vol. 9, no. 5, pp. 272–278, 2012.

[21] C. W. Song, H. Jung, and K. Chung, "Development of a medical big-data mining process using topic modeling," *Cluster Comput.*, vol. 22, no. s1, pp. 1949–1958, 2019.

[22] A. Alhudhaif, K. Polat, and O. Karaman, "Determination of COVID-19 pneumonia based on generalized convolutional neural network model from chest X-ray images," *Expert Syst. Appl.*, vol. 180, no. April, p. 115141, 2021.

[23] D. Avola, A. Bacciu, L. Cinque, A. Fagioli, M. R. Marini, and R. Taiello, "Study on transfer learning capabilities for pneumonia classification in chest-x-rays images," *Comput. Methods Programs Biomed.*, vol. 221, p. 106833, 2022.

[24] T. Pham, T. Tran, D. Phung, and S. Venkatesh, "Predicting healthcare trajectories from medical records: A deep learning approach," *J. Biomed. Inform.*, vol. 69, pp. 218–229, 2017.

[25] J. L. Gayathri, B. Abraham, M. S. Sujarani, and M. S. Nair, "A computer-aided diagnosis system for the classification of COVID-19 and non-COVID-19 pneumonia on chest X-ray images by integrating CNN with sparse autoencoder and feed forward neural network," *Comput. Biol. Med.*, vol. 141, no. December 2021, p. 105134, 2022.

[26] A. Sharma, K. Singh, and D. Koundal, "A novel fusion based convolutional neural network approach for classification of COVID-19 from chest X-ray images," *Biomed. Signal Process. Control*, vol. 77, no. April, p. 103778, 2022.

[27] F. Karim *et al.*, "Towards an effective model for lung disease classification: Using Dense Capsule Nets for early classification of lung diseases," *Appl. Soft Comput.*, vol. 124, p. 109077, 2022.

[28] F. Liu, C. Yin, X. Wu, S. Ge, P. Zhang, and X. Sun, "Contrastive Attention for Automatic Chest X-ray Report Generation," *Find. Assoc. Comput. Linguist. ACL-IJCNLP 2021*, pp. 269–280, 2021.

[29] S. R. Nayak, D. R. Nayak, U. Sinha, V. Arora, and R. B. Pachori, "Application of deep learning techniques for detection of COVID-19 cases using chest X-ray images: A comprehensive study," *Biomed. Signal Process. Control*, vol. 64, no. November 2020, p. 102365, 2021.

[30] A. Abbas, M. M. Abdelsamea, and M. M. Gaber, "Classification of COVID-19 in chest X-ray images using DeTraC deep convolutional neural network," *Appl. Intell.*, vol. 51, no. 2, pp. 854–864, 2021.